# Triple-Decker Complexes. 9.[1] Triple-Decker Complexes with Bridging Cyclopentadienyl Ligands and Novel Cyclopentadienyl Transfer Reactions†

Gerhard E. Herberich,* Ulli Englert, and Frank Marken

*Institut für Anorganische Chemie der Technischen Hochschule Aachen, Professor-Pirlet-Strasse 1, D-52056 Aachen, Germany*

Peter Hofmann*

*Anorganisch-chemisches Institut der Technischen Universität München, Lichtenbergstrasse 4, D-85747 Garching, Germany*

*Received May 26, 1993*®

The pentamethylmetallocenes CpMCp* (M = Ru, Fe) react with $[Cp^*Ru(OMe)]_2/CF_3SO_3H$ in ether to give triple-decker salts $[Cp^*M(\mu\text{-}Cp)RuCp^*]CF_3SO_3$ ($4\cdot CF_3SO_3$, M = Ru; $5\cdot CF_3SO_3$, M = Fe) with an unsubstituted Cp as the bridging ligand. The structure of $4\cdot CF_3SO_3\cdot THF$ shows average metal–ring distances of 177.6(1) pm for the outer Cp* ligands and of 185.5(1) pm for the bridging Cp ring. The metalloelectrophiles $[LM(solv)_3]^{2+}$, generated from the dichlorides $[(C_6Me_6)RuCl_2]_2$, $(Cp^*RhCl_2)_2$, $(Cp^*IrCl_2)_2$, $[(C_4Me_4)PtCl_2]_2$, and $AgCF_3SO_3$ in $MeNO_2$-$d_3$, react with CpRuCp* at room temperature to undergo novel cyclopentadienyl transfer reactions, thus forming the cations $[LMCp]^+$ besides $4^+$. With CpFeCp* labile triple-decker dications $[LMCpFeCp^*]^{2+}$ are formed in $MeNO_2$-$d_3$ at 0 °C while at higher temperature cyclopentadienyl transfer (for Ru, Ir) or alternatively redox reactions (for Rh, Pt) are observed. $[(C_6Me_5)Ru(acetone)_3](CF_3SO_3)_2$ reacts with $Fe(C_5H_4CHO)_2$ in acetone to give, after crystallization from $CHCl_3$, $[(C_6Me_6)Ru(C_5H_4CHO)]CF_3SO_3\cdot CHCl_3$ (70%). Extended Hückel MO calculations for CpFeCp* reveal weaker bonds to the Cp side and an asymmetric charge distribution with total net charges of −0.093 for the Cp and +0.104 for the Cp* fragments. This suggests that the observed regiochemistry of the stacking and ring ligand transfer reactions of **1** and **2** is primarily of electronic origin.

## Introduction

In the chemistry of triple-decker complexes three reactions are intimately connected: the formation of triple-decker complexes by electrophilic stacking of a sandwich species, the nucleophilic degradation of triple-decker complexes, and the ring ligand transfer reaction. In our previous work we have discussed the relationship between these three reactions for borole complexes and borole transfer reactions.[2,3]

In this paper we extend our studies to cyclopentadienyl systems.[4] Triple-decker complexes with bridging cyclopentadienyl ligands are still rare. The first of these, the highly reactive 34e cation $[Ni_2Cp_3]^+$,[5-7] is still the only known example with an unsubstituted bridging Cp ligand. Another important example comprises a family of robust 30e cations with a bridging pentamethylcyclopentadienyl ($C_5Me_5$ = Cp*) such as $[CpFe(\mu\text{-}Cp^*)RuCp^*]^+$ (with metal combinations as, e.g., FeRu, RuRu, and RuOs).[8,9] Our work very much relies on the results and insights gained in these pioneering studies.

We consider equilibria of type (1). These equilibria combine electrophilic stacking and nucleophilic degradation as forward and reverse reactions, respectively. If

$$LML_R + [L'M'(solv)_3]^{n+} = [LM(\mu\text{-}L_R)M'L']^{n+} + 3solv \quad (1)$$

$$[LM(\mu\text{-}L_R)M'L']^{n+} + 3solv = [L'M'L_R]^{(n-1)+} + [LM(solv)_3]^+ \quad (2)$$

LM = CpFe, CpRu, Cp*Fe, Cp*Ru

$L_R$ = Cp

$L'M'^{n+}$ = $(C_6Me_6)Ru^{2+}$, $Cp^*Ru^+$, $Cp^*Rh^{2+}$, $Cp^*Ir^{2+}$, $(C_4Me_4)Pt^{2+}$

solv = $C_6H_6$, MeCN (AN), $Me_2CO$, $MeNO_2$

the two complex fragments LM and L'M' are different there is a choice for the regiochemistry of the nucleophilic

† Dedicated to Professor Heinrich Nöth on the occasion of his 65th birthday.

® Abstract published in *Advance ACS Abstracts,* September 1, 1993.

(1) Part 8: Herberich, G. E.; Köffer, D. P. J.; Peters, K. M. *Chem. Ber.* **1991,** *124,* 1947.

(2) Herberich, G. E.; Dunne, B. J.; Hessner, B. *Angew. Chem., Int. Ed. Engl.* **1989,** *28,* 737.

(3) Herberich, G. E.; Büschges, U.; Dunne, B. J.; Hessner, B.; Klaff, N.; Köffer, D. P. J.; Peters, K. M. *J. Organomet. Chem.* **1989,** *372,* 53.

(4) Marken, F. Dissertation, Technische Hochschule Aachen, 1992.

(5) Werner, H.; Salzer, A. *Synth. Inorg. Met.-Org. Chem.* **1972,** *2,* 239. Salzer, A.; Werner, H. *Synth. Inorg. Met.-Org. Chem.* **1972,** *2,* 249. Salzer, A.; Werner, H. *Angew. Chem., Int. Ed. Engl.* **1972,** *11,* 930. Werner, H.; Ulrich, B.; Salzer, A. *J. Organomet. Chem.* **1977,** *141,* 339.

(6) Dubler, E.; Textor, M.; Oswald, H. R.; Jameson, G. B. *Acta Crystallogr.* **1983,** *B39,* 607.

(7) Werner, H. *Angew. Chem., Int. Ed. Engl.* **1977,** *16,* 1.

(8) Kudinov, A. R.; Rybinskaya, M. I.; Struchkov, Yu. T.; Yanovskii, A. I.; Petrovskii, P. V. *J. Organomet. Chem.* **1987,** *336,* 187.

(9) Lumme, P. O.; Turpeinen, U.; Kudinov, A. R.; Rybinskaya, M. I. *Acta Crystallogr.* **1990,** *C46,* 1410.

0276-7333/93/2312-4039$04.00/0 

**Scheme I**

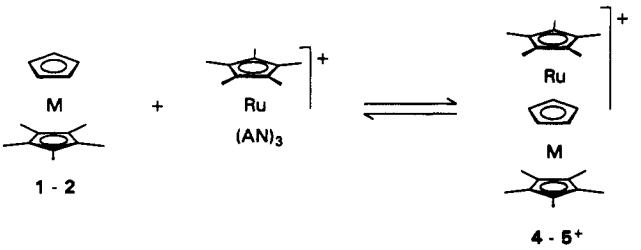


[a] Key: 1, M = Ru; 2, M = Fe; $4^+$, M = Ru; $5^+$, M = Fe; AN = MeCN.

degradation and a second equilibrium (2) comes into play. The combination of (1) and (2) may result in a transfer of the ring ligand $L_R$ from M to M′.

## Monocationic Triple-Decker Complexes with a Bridging Cyclopentadienyl Ligand

Pentamethylruthenocene CpRuCp* (1)[8,10,11] was prepared from $(RuClCp^*)_4$/NaCp·DME, and its ferrocene analogue CpFeCp* (2) by a modified literature procedure from ref 12. When 1 and 2 are treated with $[Cp^*Ru(AN)_3]^+$ (3)[8] in acetone, two new triple-decker cations $[Cp^*Ru(\mu\text{-}Cp)RuCp^*]^+$ ($4^+$) and $[Cp^*Fe(\mu\text{-}Cp)RuCp^*]^+$ ($5^+$) appear in an equilibrium of electrophilic stacking and nucleophilic degradation reactions, respectively (Scheme I). In an NMR tube experiment the conversion of 1 and 2 to $4^+$ and $5^+$ reached about 30 %. When 1 equiv of benzene was added, the triple-decker complexes disappeared and the cation $[Cp^*Ru(C_6H_6)]^+$ [8] was formed. Cation $5^+$ slowly decays in the dark and rapidly in daylight to produce 1 and presumably $[Cp^*Fe(solv)_3]^+$, leading to unidentified paramagnetic decomposition products; decamethylferrocene was not detected in the $^1H$ NMR spectrum. It is important to note that the formation of 1 comprises the transfer of the unsubstituted cyclopentadienyl ligand from the iron center in 2 to the ruthenium center in 1.

The position of the equilibrium of Scheme I depends on the nature of the ligands present. While benzene shifts the equilibrium to the left, thus effecting complete degradation of $4^+$ and $5^+$, solvents with weaker ligand properties such as acetone, ether, dichloromethane, and nitromethane favor triple-decker formation. Likewise, coordinating counterions effect nucleophilic degradation and have to be avoided if the synthesis of a triple-decker complex is intended. The combination $[Cp^*Ru(OMe)]_2$/$CF_3SO_3H$ in ether[13,14] can serve as an efficient source of the $Cp^*Ru^+$ fragment under highly nonnucleophilic conditions. Thus, stacking of 1 and 2 with this reagent produces the triple-decker salts $4\cdot CF_3SO_3$ with two Ru centers and $5\cdot CF_3SO_3$ with the FeRu combination. The byproduct $[(Cp^*Ru)_3(OMe)_2]CF_3SO_3$[14] can readily be separated because of its greater solubility. Both salts can be crystallized from $CHCl_3$ or THF as solvates with one weakly bound solvent molecule which is lost slowly after isolation of the crystals.

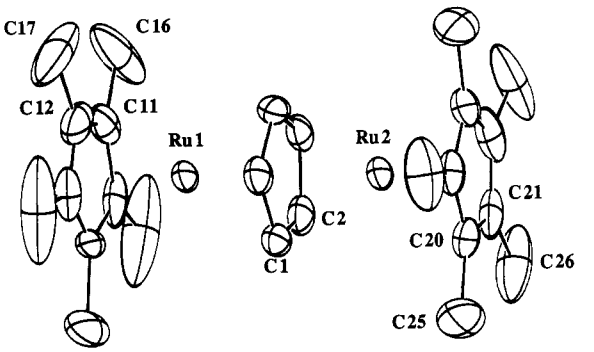


**Figure 1.** Structure of the cation of $4\cdot CF_3SO_3\cdot THF$.

The stacking reactions of Scheme I show a remarkable regioselectivity: Stacking occurs exclusively at the unsubstituted cyclopentadienyl ring. For $4^+$ this is readily deduced from the $^1H$ NMR spectrum which shows only two signals with intensities 30 (2 Cp*):5 ($\mu$-Cp). We note here that the known cation of $[CpRu(\mu\text{-}Cp^*)RuCp^*]PF_6$[8] is an isomer of $4^+$. Both cations $4^+$ and $5^+$ show the $^1H$ and $^{13}C$ NMR signals for the Cp ligand at remarkably high field [$\delta(^1H)$ 4.47 (acetone-$d_6$) for $4^+$, 4.22 (acetone-$d_6$) for $5^+$, 4.7 ($MeNO_2$-$d_3$) for $[Ni_2Cp_3]^+$;[5] $\delta(^{13}C)$ 57.7 for $4^+$, 56.4 for $5^+$]. These observations also prove the presence of the Cp ligand in the bridging position. Thus, the two cations are the second and third examples of a triple-decker complex with an unsubstituted $\mu$-Cp ring.

We have also tested the reactivity of the unsubstituted metallocenes. Ferrocene reacts with $[Cp^*Ru(AN)_3]CF_3SO_3$ in acetone-$d_6$ at 60 °C to give CpRuCp* (1) in a remarkably slow cyclopentadienyl transfer reaction. After 24 h only signals of 1, free acetonitrile, and unconsumed ferrocene are seen in the NMR spectrum. Under the same conditions ruthenocene shows only 10% conversion after 72 h while with osmocene no reaction could be detected.

## Structure of $[Cp^*Ru(\mu\text{-}Cp)RuCp^*]CF_3SO_3\cdot THF$

Yellow crystals of $4\cdot CF_3SO_3\cdot THF$ were obtained from THF solutions at about −30 °C. The structure was determined by X-ray crystallography (Figure 1 and Tables I and II). Two problems were encountered. The triflate anion occupies two sites with similar multiplicities of 0.6 and 0.4. The distances within the anions indicate some disorder. The presence of one THF molecule was confirmed by $^1H$ NMR spectroscopy, and a difference Fourier synthesis showed local maxima of electron density near the sites occupied partially by the anion. Close to the position with lower anion multiplicity, the electron density maxima could be interpreted as a five-membered ring. Free refinement of the solvent molecule was not possible, but inclusion of a rigid model in structure factor calculations reduced $R_w$ from 0.071 to 0.056; for the subset of observed reflections with low Bragg angles the improvement was very pronounced.

The cation shows a typical triple-decker structure. The averaged Ru–C distance amounts to 213.7 pm for the outer Cp* and 222.2 pm for the bridging $\mu$-Cp ligand. This difference is more pronounced than for $[Ru_2Cp^*_3]PF_6$[9] [with 216 pm for the outer Cp* and 220 pm for the $\mu$-Cp* ligand].

Two effects are operating here. The structures of triple-decker complexes with three identical ring ligands show that metal-to-ligand bonding is generally weaker for the central ligand as compared to the outer ligands. Pertinent

(10) Albers, M. O.; Liles, D. C.; Robinson, D. J.; Shaver, A.; Singleton, E.; Wiege, M. B.; Boeyens, J. C. A.; Levendis, D. C. *Organometallics* **1986**, *5*, 2321.
(11) Zanin, I. E.; Antipin, M. Yu.; Struchkov, Yu. T. *Kristallografiya* **1991**, *36*, 430; *Sov. Phys. Crystallogr.* **1991**, *36*, 225.
(12) Bunel, E. E.; Valle, L.; Manriquez, J. M. *Organometallics* **1985**, *4*, 1680.
(13) Koelle, U.; Wang, M. H. *Organometallics* **1990**, *9*, 195.
(14) Koelle, U.; Kossakowski, J.; Boese, R. *J. Organomet. Chem.* **1989**, *378*, 449.

**Table I. Non-Hydrogen Atom Coordinates for $4{\cdot}CF_3SO_3{\cdot}THF$**

| atom | x | y | z | $B_{eq}$[a] |
|---|---|---|---|---|
| Ru1 | 0.34602(5) | 0.11613(4) | 0.25425(5) | 4.08(1) |
| Ru2 | 0.22559(5) | 0.31921(4) | 0.11598(5) | 4.19(1) |
| S1 | -0.0941(4) | 0.1071(4) | 0.2077(5) | 8.5(2) |
| S2 | 0.6203(5) | 0.4175(6) | 0.3218(6) | 8.1(2) |
| F11 | -0.108(1) | 0.204(1) | 0.446(1) | 13.4(5) |
| F12 | -0.078(2) | 0.068(1) | 0.395(1) | 22.6(7) |
| F13 | 0.031(1) | 0.170(1) | 0.419(2) | 17.9(7) |
| F21 | 0.742(2) | 0.575(1) | 0.377(2) | 14.2(7) |
| F22 | 0.7800(9) | 0.428(1) | 0.235(1) | 8.9(4) |
| F23 | 0.813(1) | 0.476(1) | 0.427(2) | 15.1(7) |
| O11 | -0.036(1) | 0.017(1) | 0.153(2) | 13.8(6) |
| O12 | -0.043(1) | 0.210(1) | 0.249(2) | 21.6(7) |
| O13 | -0.191(1) | 0.085(2) | 0.193(2) | 21.6(8) |
| O21 | 0.583(2) | 0.463(2) | 0.435(1) | 10.7(6) |
| O22 | 0.582(3) | 0.396(2) | 0.196(2) | 11.3(7) |
| O23 | 0.636(3) | 0.297(2) | 0.263(3) | 18(1) |
| C1 | 0.3368(6) | 0.2950(6) | 0.2804(7) | 5.3(2) |
| C2 | 0.3680(6) | 0.2256(5) | 0.1521(7) | 4.9(2) |
| C3 | 0.2838(6) | 0.1446(6) | 0.0703(7) | 5.1(2) |
| C4 | 0.1992(6) | 0.1619(6) | 0.1446(7) | 4.8(2) |
| C5 | 0.2335(6) | 0.2548(5) | 0.2708(7) | 4.5(2) |
| C6 | -0.064(2) | 0.127(3) | 0.351(2) | 27.1(9) |
| C7 | 0.754(2) | 0.460(2) | 0.312(2) | 6.6(5)* |
| C10 | 0.4726(6) | 0.0058(6) | 0.2608(8) | 6.6(2) |
| C11 | 0.3813(9) | -0.0579(6) | 0.2170(8) | 8.3(3) |
| C12 | 0.3211(7) | -0.0205(6) | 0.3090(8) | 7.0(2) |
| C13 | 0.3701(7) | 0.0685(6) | 0.4161(7) | 6.6(2) |
| C14 | 0.4727(7) | 0.0904(6) | 0.3908(8) | 6.9(2) |
| C15 | 0.555(1) | -0.020(1) | 0.177(1) | 19.7(4) |
| C16 | 0.352(1) | -0.1604(9) | 0.084(1) | 20.0(7) |
| C17 | 0.212(1) | -0.075(1) | 0.285(1) | 18.7(5) |
| C18 | 0.331(1) | 0.131(1) | 0.542(1) | 19.3(4) |
| C19 | 0.552(1) | 0.1751(9) | 0.487(1) | 23.0(5) |
| C20 | 0.2212(7) | 0.4939(6) | 0.1442(8) | 6.7(2) |
| C21 | 0.2556(7) | 0.4294(7) | 0.0273(8) | 7.7(2) |
| C22 | 0.1701(8) | 0.3484(6) | -0.0590(7) | 6.7(2) |
| C23 | 0.0856(6) | 0.3651(6) | 0.0101(8) | 5.7(2) |
| C24 | 0.1179(7) | 0.4538(6) | 0.1365(8) | 6.2(2) |
| C25 | 0.285(1) | 0.5895(8) | 0.260(1) | 14.3(4) |
| C26 | 0.3580(9) | 0.4444(9) | -0.007(1) | 15.4(3) |
| C27 | 0.164(1) | 0.2584(9) | -0.2015(9) | 12.4(4) |
| C28 | -0.0219(8) | 0.2988(8) | -0.042(1) | 11.8(4) |
| C29 | 0.0585(9) | 0.5046(9) | 0.244(1) | 12.8(4) |
| O9 | 0.595(1) | 0.488(2) | 0.308(1) | 23.3(7)* |
| C91 | 0.674 | 0.578 | 0.362 | 23.3* |
| C92 | 0.774 | 0.537 | 0.426 | 23.3* |
| C93 | 0.750 | 0.416 | 0.412 | 23.3* |
| C94 | 0.632 | 0.397 | 0.341 | 23.3* |

[a] The anisotropic thermal parameters are given in the form of their isotropic equivalents defined as $(4/3)[a^2\beta_{11} + b^2\beta_{22} + c^2\beta_{33} + ac(\cos\beta)\beta_{13}]$; in $10^4$ pm$^2$. Starred values refer to atoms that were treated isotropically.

structural data are available for $[Ni_2Cp_3]BF_4$,[6] $Cr_2(1,3,5\text{-}C_6H_3Me_3)_3$,[15] $Co_2(C_4H_4BMe)_3$,[16] $[Ru_2Cp^*_3]PF_6$,[9] and $Co_2Cp^*_3$.[17] This behavior is in accord with the bonding situation in triple-decker complexes.[18] The second effect stems from the different bonding properties of the cyclopentadienyl ligands Cp and Cp*. The structure of the unsymmetric ruthenocene **1** shows a structural trans effect: Its Cp* ring is more tightly bonded with Ru–C(av) 217.6 pm than its Cp ring with Ru–C(av) 219.6 pm at 123 K.[11] The same is true for the unsymmetric ferrocene **2** where a recent variable temperature structure investigation gave Fe–C(av) 204.1 pm for the permethylated ring and 205.1 pm for the unsubstituted ring; the difference of 1.0(3) pm is smaller than in the ruthenocene case but still significant.[19] The same effect also operates in $4^+$ and strengthens the Ru–Cp* bond of the outer ligands and weakens the Ru–($\mu$-Cp) bond of the bridging $\mu$-Cp ligand in comparison to $[Ru_2Cp^*_3]^+$. We will come back to this point below.

**Table II. Selected Bond Distances (pm) for $4{\cdot}CF_3SO_3{\cdot}THF$**

| | | | |
|---|---|---|---|
| Ru1–Cp | 185.7(1) | Ru2–Cp | 185.3(1) |
| Ru1–C1 | 220.5(7) | Ru2–C1 | 222.1(7) |
| Ru1–C2 | 221.9(6) | Ru2–C2 | 221.2(6) |
| Ru1–C3 | 223.7(7) | Ru2–C3 | 222.7(6) |
| Ru1–C4 | 223.4(6) | Ru2–C4 | 223.4(7) |
| Ru1–C5 | 222.3(6) | Ru2–C5 | 220.8(6) |
| Ru1–Cp*$_1$ | 178.0(1) | Ru2–Cp*$_2$ | 177.2(1) |
| Ru1–C10 | 212.6(7) | Ru2–C20 | 214.4(7) |
| Ru1–C11 | 215.4(8) | Ru2–C21 | 213.5(8) |
| Ru1–C12 | 215.0(7) | Ru2–C22 | 213.6(7) |
| Ru1–C13 | 211.8(7) | Ru2–C23 | 215.1(7) |
| Ru1–C14 | 211.7(7) | Ru2–C24 | 214.1(7) |

**Scheme II**

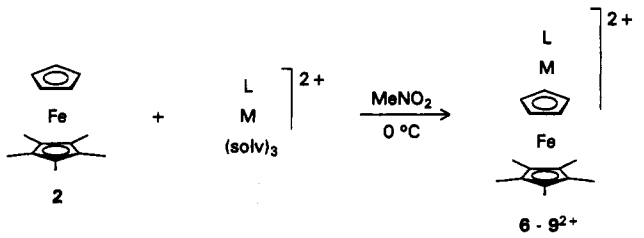


[a] Key: $6^{2+}$, LM = $(C_6Me_6)Ru$; $7^{2+}$, LM = Cp*Rh; $8^{2+}$, LM = Cp*Ir; $9^{2+}$, LM = $(C_4Me_4)Pt$.

**Table III. $^1$H NMR Data for $6\text{–}9^{2+}$ and $10\text{–}13^+$**

| | |
|---|---|
| $[(C_6Me_6)Ru(solv)_3]^+$ [b] | 2.27 |
| $6^{2+}$ [c] | 2.41 ($C_6Me_6$), 4.98 (Cp), 1.92 (FeCp*) |
| $10^+$ [d] | 2.48 ($C_6Me_6$), 5.17 (Cp) |
| $[Cp^*Rh(solv)_3]^+$ [b] | 1.74 |
| $7^{2+}$ [c] | 2.09 (RhCp*), 5.15 (Cp), 1.93 (FeCp*) |
| $11^+$ [d] | 2.19(RhCp*), 5.71 (Cp) |
| $[Cp^*Ir(solv)_3]^+$ [b] | 1.66 |
| $8^{2+}$ [c] | 2.21(IrCp*), 5.09 (Cp), 1.98 (FeCp*) |
| $12^+$ [b] | 2.27 (IrCp*), 5.60 (Cp) |
| $[(C_4Me_4)Pt(solv)_3]^+$ [b,e] | 1.77 (25) |
| $9^{2+}$ [c,e] | 2.85(16) ($C_4Me_4$), 4.70 (Cp), 1.90 (FeCp*) |
| $13^+$ [b,e] | 2.33 (26) ($C_4Me_4$), 6.19 (26) (Cp) |

[a] Measured at 80 MHz vs internal TMS. [b] In $MeNO_2$-$d_3$ at ambient temperature. [c] In $MeNO_2$-$d_3$ at 0 °C. [d] In $Me_2CO$-$d_6$ at ambient temperature. [e] $J(^{195}Pt\text{–}^1H)$ coupling constants in parentheses.

## Dicationic Triple-Decker Complexes with a Bridging Cyclopentadienyl Ligand

In further exploratory work we have tested the interaction of **1** and **2** with dicationic metalloelectrophiles which were generated from the dichlorides $[(C_6Me_6)RuCl_2]_2$, $(Cp^*RhCl_2)_2$, $(Cp^*IrCl_2)_2$, and $[(C_4Me_4)PtCl_2]_2$ and $AgCF_3SO_3$ in $MeNO_2$-$d_3$. At temperatures not higher than 0 °C CpFeCp* (**2**) formed deeply colored triple-decker cations $6^{2+}$ (dark green), $7^{2+}$ (blue), $8^{2+}$ (blue), and $9^{2+}$ (red) (Scheme II). In the $^1$H NMR spectra of these species the signal of the Cp ligand appears at lower field than for the monocations $4^+$ and $5^+$ but still at higher field than for the comparable sandwich cations $10\text{–}13^+$ with the same central metal and a terminal Cp ligand (Table III). The signal of the Cp*Fe group is found in a narrow range at $\delta$ 1.90–1.98, which also includes the

(15) Lamanna, W. M.; Gleason, W. B.; Britton, D. *Organometallics* **1987**, *6*, 1583.
(16) Herberich, G. E.; Hessner, B.; Saive, R. *J. Organomet. Chem.* **1987**, *319*, 9.
(17) Schneider, J. J.; Goddard, R.; Werner, S.; Krüger, C. *Angew. Chem., Int. Ed. Engl.* **1991**, *30*, 1124.
(18) Lauher, J. W.; Elian, M.; Summerville, R. H.; Hoffmann, R. *J. Am. Chem. Soc.* **1976**, *98*, 3219.
(19) Zanin, I. E.; Antipin, M. Yu.; Struchkov, Yu. T.; Kudinov, A. R.; Rybinskaya, M. I. *Metalloorg. Khim.* **1992**, *5*, 579.

**Scheme III**

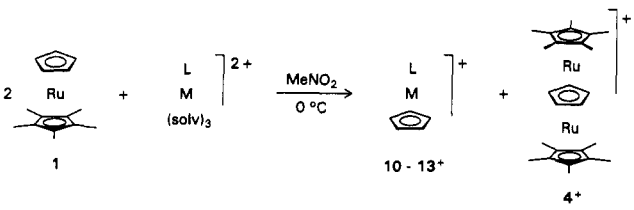


[a] Key: $10^+$, $[LMCp]^+ = [CpRu(C_6Me_6)]^+$;[21] $11^+$, $[LMCp]^+ = [CpRhCp^*]^+$;[22] $12^+$, $[LMCp]^+ = [CpIrCp^*]^+$;[22] $13^+$, $[LMCp]^+ = [CpPt(C_4Me_4)]^+$.[20]

chemical shift value for $5^+$ ($\delta$ 1.95), while bridging ($\mu$-Cp*)Fe groups would show a low-field shift ($\delta$ ca. 2.6; cf. ref 8). Thus both arguments lead to the same conclusion: The new species $6$–$9^{2+}$ all possess an unsubstituted $\mu$-Cp ligand.

At higher temperatures decomposition takes place. In the cases of $6^{2+}$ and $8^{2+}$ ring ligand transfer with formation of the sandwich cations $10^+$ and $12^+$ is observed while in the cases of $7^{2+}$ and $9^{2+}$ redox reactions with formation of $2^+$ seem to take place as inferred from the developing green color and paramagnetism of the solutions. When ferrocene is used instead of **2**, no triple-decker species are seen at 0 °C and the analogous cyclopentadienyl transfer reactions and redox reactions are much slower.

CpRuCp* (**1**) is much less prone to redox reactions. In all cases Cp transfer is observed in $MeNO_2$-$d_3$ and sandwich cations $10$–$13^+$ are formed (Scheme III). The same is true in acetone-$d_6$ with the exception of the labile platinum species $[(C_4Me_4)Pt(acetone)_x]^{2+}$ [20] where no Cp transfer could be detected. The $[Cp^*Ru(solv)_3]^+$ fragment liberated in the course of the ring ligand transfer reaction consumes a second equivalent of **1** and forms the triple-decker cation $4^+$. Therefore 2 equiv of **1** appear in the resulting overall reaction (Scheme III). We note that less reactive species of the type $[Cp^*Ru(solv)_3]^+$ such as $[Cp^*Ru(NCMe)_3]^+$ [8] are well characterized whereas the number of coordinated solvent molecules in the present case (solv = $MeNO_2$ or acetone) is only presumed from analogy.

Ruthenocene is again much less reactive than its pentamethyl derivative **1**, and ring ligand transfer was observed for the rhodium and iridium electrophiles only.

As an example for a synthetic application of Cp transfer reactions we treated $Fe(C_5H_4CHO)_2$ with $[(C_6Me_6)Ru(acetone)_3]^{2+}$ at room temperature. Workup after 24 h and crystallization from chloroform gave the new complex $[(C_6Me_6)Ru(C_5H_4CHO)]CF_3SO_3$ (**14**) as solvate **14**·$CHCl_3$ in good yield.

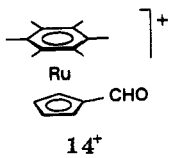


$14^+$

## Bonding and Electronic Structure/Reactivitiy Considerations

The remarkable regioselectivity of triple-decker formation reactions with their exclusive stacking on top of the Cp ligand of **1** and **2** and the observed preference for Cp vs Cp* transfer processes deserve some further comments.

On the basis of extended Hückel MO model calculations[23] we therefore turn to some electronic structure considerations, which seem relevant for bonding and reactivity patterns of unsymmetric metallocenes such as CpRuCp* (**1**) and CpFeCp* (**2**).

As mentioned above, the available X-ray structure determinations (at different temperatures) for **1**[11] and **2**[19] clearly reveal a static structural trans effect, which must be entirely due to the pentamethyl substitution of one cyclopentadienyl ligand. Consistently and beyond experimental error, the M–Cp distances in **1** and **2** are found to be longer than their M–Cp* counterparts. If one accepts the normal correlation of larger bond distances with weaker bonds (in a thermochemical and kinetic sense), then the static structural differences in M–Cp and M–Cp* bonding should reflect related electronic differences in M–Cp and M–Cp* interactions.[24] Their understanding seems important in the context of explaining CpMCp* stacking and ligand transfer reactions of **1** and **2** and ought to be transferable to $4^+$ and its congeners.

In order to discuss the bonding situation of **1** and **2** in a general, qualitatively transparent way, the extended Hückel MO method, combined with perturbation arguments and fragment MO calculations[25] seems appropriate. It should be noted that any numerically accurate computation for **1** or **2**, attempting to correctly reproduce, e.g., their precise experimental ground state structures, would require large basis set ab initio calculations with highly correlated wavefunctions or analogous approaches as well as complete geometry optimization, as amply documented for the famous ferrocene case and related systems in the past.[26] Although standard extended Hückel calculations often do not allow reliable distance optimizations, we parenthetically note here that for the parent systems $FeCp_2$ and $RuCp_2$ the mininum energy is found for reasonable values of 202 (Fe) and 207 pm (Ru, slightly too short) for the metal-to-carbon distances, if the metal–Cp separation is optimized in $D_{5d}$ or $D_{5h}$ symmetry, in accord with our earlier experiences with $ML_n$ complexes or cyclic $\pi$-systems.[27] As expected, however, the potential energy surface in the vicinity of the minimum is extremely soft[28] and does not allow a meaningful computational prediction of minimally different M–Cp and M–Cp* distances, if CpFeCp* and CpRuCp* are both minimized

(20) Herberich, G. E.; Englert, U.; Marken, F. *J. Chem. Soc., Dalton Trans.* **1993**, 1979.
(21) Robertson, I. W.; Stephenson, T. A.; Tocher, D. A. *J. Organomet. Chem.* **1982**, *228*, 171.
(22) Moseley, K.; Kang, J. W.; Maitlis, P. M. *J. Chem. Soc. A* **1970**, 2875.
(23) Hoffmann, R. *J. Chem. Phys.* **1963**, *39*, 1397.
(24) For earlier comments on the different bonding properties of Cp and Cp* ligands see: (a) Calabro, D. C.; Hubbard, J. L.; Blevins, C. H., II; Campbell, A. C.; Lichtenberger, D. L. *J. Am. Chem. Soc.* **1981**, *103*, 6839. (b) Koelle, U.; Khouzami, F. *Angew. Chem., Int. Ed. Engl.* **1980**, *19*, 640. (c) Robbins, J. L.; Edelstein, N.; Spencer, B.; Smart, J. C. *J. Am. Chem. Soc.* **1982**, *104*, 1882. (d) Gassman, P. G.; Mickelson, J. W.; Sowa, J. R., Jr. *J. Am. Chem. Soc.* **1992**, *114*, 6942. (e) Ryan, M. F.; Siedle, A. R.; Burk, M. J.; Richardson, D. E. *Organometallics* **1992**, *11*, 4231. (f) Richardson, D. E.; Ryan, M. F.; Khan, Md. N. I.; Maxwell, K. A. *J. Am. Chem. Soc.* **1992**, *114*, 10482.
(25) For a general introduction see: Albright, T. A.; Burdett, J. K.; Whangbo, M.-H. *Orbital Interactions in Chemistry*; Wiley: New York, 1985.
(26) (a) Haaland, A. *Acc. Chem. Res.* **1979**, *12*, 415. (b) Coutière, M.-M.; Demuynck, J.; Veillard, A. *Theor. Chim. Acta* **1972**, *27*, 281. (c) Bagus, P. S.; Almlof, J. *J. Chem. Phys.* **1976**, *64*, 2324. Ammeter, J. H.; Bürgi, H.-B.; Thiebeault, J. C.; Hoffmann, R. *J. Am. Chem. Soc.* **1978**, *100*, 3686.
(27) (a) Albright, T. A.; Hofmann, P.; Hoffmann, R. *J. Am. Chem. Soc.* **1977**, *99*, 7546. (b) Albright, T. A.; Hofmann, P.; Hoffmann, R.; Lillya, C. P.; Dobosh, P. A. *J. Am. Chem. Soc.* **1983**, *105*, 3396.
(28) A deviation of 5 pm for, e.g., the Fe–C distance of $FeCp_2$ costs less than 4 kcal/mol.

**Scheme IV**

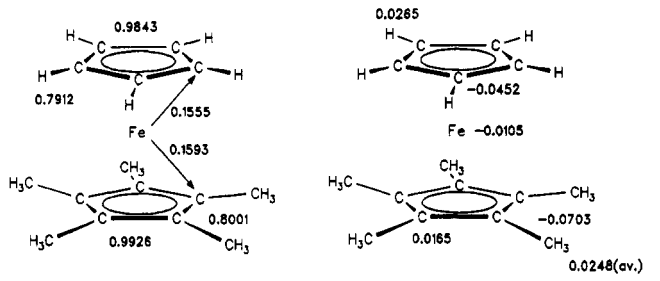


with respect to their two independent metal–ring separations (remember that we are dealing with experimental bond length variations in the 1–3-pm range). Without resorting to the ultimate choice of ab initio theory at the required level of sophistication, a different approach was taken. A fixed geometry[29] for the mixed iron compound **2** was used as a model, with all Fe–$C_{ring}$ distances set equal to 205 pm. This allows us to make use of the computed differences in overlap populations, charges, etc. to tell us about the different bonding of the metal to either ring. A simple electronic picture of the observed trans effect will emerge from this.

In Scheme IV we display the computed reduced overlap populations as well as the atomic net charges for CpFeCp* (Mulliken population analysis), as they evolve for the above model geometry based upon experimental data but with both distances Fe–$Cp_{center}$ set to 165 pm (making all Fe–C bonds 205 pm).

Apparently, there is a distinct difference between the metal–ring interactions on both sides, which is most obvious from the net atomic charges of the Cp and the Cp* carbon atoms. While they carry a negative overall charge (−0.0452) in the cyclopentadienyl ring, they possess a small positive charge (+0.0165) in the permethylated system. Together with the hydrogen values this leads to a total fragment charge of the Cp moiety of −0.093 in an FMO calculation, compared to +0.104 for the entire Cp* fragment. The metal center remains practically neutral. The reduced overlap populations between the iron atom and the ring carbons (a direct measure of Fe–C bonding interactions) are slightly larger toward the Cp* ligand which, on the other hand, displays the larger C–C overlap populations within the ring skeleton. As to Fe–C bonding, the trend indicated by the model calculation for the fully idealized CpFeCp* system thus reflects the structural observations for **1** and **2** mentioned above, i.e. the shorter bonds toward the Cp* carbons. The larger C–C overlap populations for the pentamethyl substituted ring of Scheme IV, however, seem to contradict the experimental data for **1**[11] and **2**,[19] because slightly longer averaged carbon–carbon distances seem to prevail in the Cp* ligand in each case. If we, however, compare the numbers for Cp (0.984) and Cp* (0.993) of CpFeCp* in Scheme IV with the corresponding values of free $Cp^-$ and $Cp^{*-}$ (for the same geometries with identical C–C distances), we find reduced overlap populations of 1.0457 and 1.0575, respectively, i.e. an intrinsically larger value for $Cp^{*-}$ due to the methyl substitution and independent of any interaction with the metal. According to the numbers in Scheme IV, coordination to the metal not only causes C–C bond lengthening for both rings but also points to a somewhat more pronounced weakening within the Cp* ring.

Overall, a picture emerges from the CpFeCp* model which reveals weaker bonds from the metal to the Cp side and an asymmetric charge distribution that makes the weaker donating ("more electronegative"[30]) Cp ligand the negative end of the CpFeCp* dipole. The analysis of this effect is rather straightforward.

If we compare the free ligands $Cp^-$ and $Cp^{*-}$, the consequence of the pentamethyl substitution upon the relevant $\pi$-MOs of $Cp^-$ is shown in Scheme V (left side).

All $\pi$-levels are destabilized significantly for $Cp^{*-}$, and this in turn must lead to inequivalent metal–ring interactions for Fe–Cp* vs Fe–Cp. In addition, the $\pi$-orbitals of $Cp^{*-}$ to a certain extent are delocalized over the five methyl groups. When we want to describe these interactions for CpFeCp* in an analogous manner to the well-known standard case of ferrocene, i.e. by constructing the usual interaction diagram[31] between $Fe^{2+}$ and the appropriate linear combinations of $\pi$-orbitals for the two ligands, the orbital set of the $[Cp_2]^{2-}$ fragment of ferrocene has to be replaced by that of a $[CpCp^*]^{2-}$ unit. The energetic consequences for going from $[Cp_2]^{2-}$ to $[CpCp^*]^{2-}$ are displayed qualitatively on the right side of Scheme V for a ring–ring distance of 330 pm as used in the CpFeCp* model. The fully delocalized, symmetry-adapted linear combinations of $\pi$-MOs for the $[Cp_2]^{2-}$ fragment of ferrocene, with identical contributions to the wavefunctions on both rings, are being replaced by $\pi$-MO linear combinations of the $[CpCp^*]^{2-}$ unit which, due to the different $\pi$-MO energies of $Cp^-$ and $Cp^{*-}$, are energetically much more disperse and become heavily localized on either the Cp or the Cp* subunit. In an actual fragment MO calculation for **2** we find this localization within the ligand fragment $[CpCp^*]^{2-}$ to be 85–90%, and the $\pi$-orbitals in Scheme V have been assigned accordingly as either Cp– or Cp*-based. As expected from the $Cp^-$ to $Cp^{*-}$ comparison, the lower lying $\pi$-MOs of each set carry predominant Cp character. Interacting the $[CpCp^*]^{2-}$ $\pi$-system with the metal center leads to more charge transfer (back-bonding) from $d_{x^2-y^2}$ and $d_{xy}$ of Fe to the $3\pi$-orbital set of $Cp^-$ (0.165 e) than to $3\pi$ of $Cp^{*-}$ (0.032 e), due to the lower energy of the $3\pi$ acceptor levels of the cyclopentadienyl ligand. On the other hand, the $2\pi$ set of $Cp^-$ (fully occupied with 2 e for the free ligand $Cp^-$) retains more electrons (1.734 e) than the better donor levels $2\pi$ of $Cp^{*-}$ (1.224 e). The opposite trend is seen for $1\pi$ of both competing ligands (1.836 e for $Cp^-$, 1.914 e for $Cp^{*-}$), but to a much smaller extent. Here $1\pi$ of $Cp^-$ loses more electrons than $1\pi$ of $Cp^{*-}$ due to its better overlap with the appropriate metal orbitals ($1\pi$ of $Cp^{*-}$ is spread out over the methyl groups, and their $CH_3$ group orbitals of $\pi$-symmetry mix into $1\pi$ of $Cp^{*-}$ in an antibonding sense, reducing the overall overlap to the iron center). As the main bonding interaction between the metal and the rings comes from the interaction of $d_{xz}$ and $d_{yz}$ with the $2\pi$ set of the cyclic ligands, the higher lying and thus much better $\pi$-donor levels $2\pi$ of $Cp^{*-}$ cause stronger bonding from the metal to the carbons of the pentamethyl substituted ring and,

(29) The following geometrical parameters were used: all Fe–C = 205 pm, all C–C = 144 pm, all C–H = 110 pm, C–$C_{Me}$ = 150 pm; Cp ring, $D_{5h}$; Cp*, $C_{5v}$ with methyl carbons in the ring plane and one methyl hydrogen orientated toward Fe.

(30) For an assignment of substituent parameters for Cp derivatives from gas phase electron transfer studies see ref 24e.

(31) See for example ref 25, p 393.

**Scheme V**

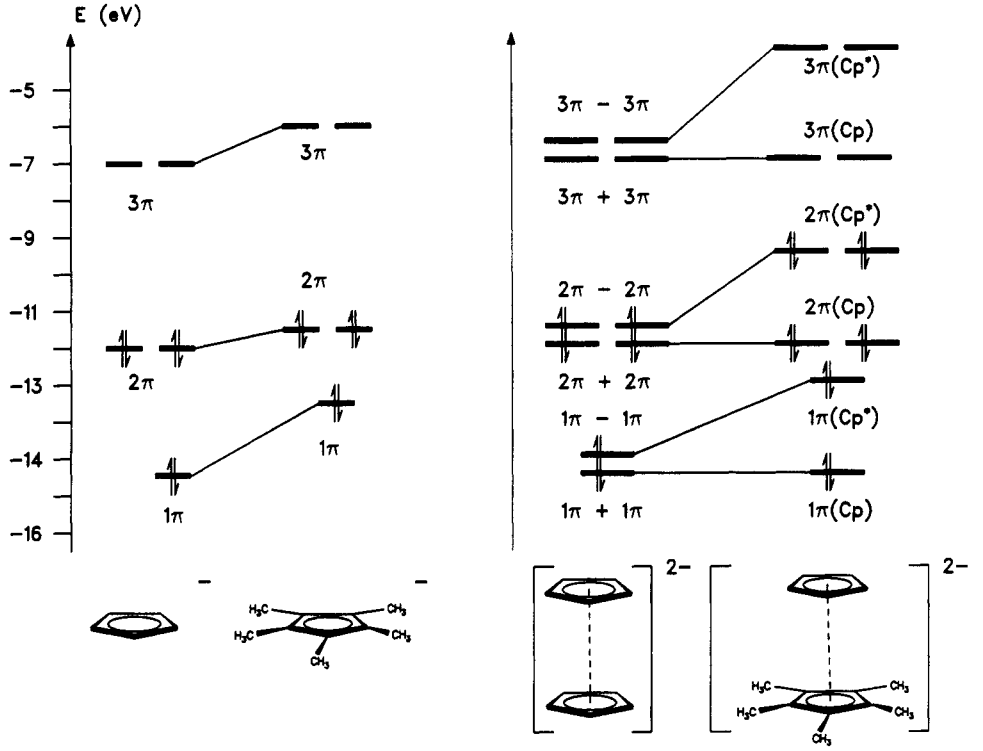


as a corollary, the weaker donating $Cp^-$ ligand keeps more of its electron density in its $2\pi$-level set. The above mentioned slightly more effective $\delta$-type back-bonding to the lower lying $3\pi$ acceptor MOs of $Cp^-$ augment this trend further.

The overall situation is similar to a simple linear triatomic A–M–X, with X (A) being the more (less) electronegative substituent of M, the negative (positive) end of the A–M–X dipole, and the better (worse) leaving group.[32]

Referring back to the chemistry of triple-decker formation and to the regioselectivity of stacking and ligand transfer processes described earlier in this paper, the electronic differences between $Cp^-$ and $Cp^{*-}$ ligands, in line with the results of our model calculations, can explain the experimental reactivity and structure observations in a satisfactory manner. Extensions to related systems, including, e.g., triple-decker complexes like $4^+$ or different arene substitution patterns of arene ligands, seem obvious.

## Conclusions

The pentamethylmetallocenes **1** and **2** show a remarkable regioselectivity in electrophilic stacking reactions. In the new triple-decker cations $4^+$, $5^+$, and $6$–$9^{2+}$ the bridging ligand is always the unsubstituted cyclopentadienyl ring. In the related cyclopentadienyl transfer reactions the migrating cyclopentadienyl is again always the unsubstituted ligand. This can be understood on the basis of electronic structure differences between $Cp^-$ and $Cp^{*-}$, brought about by pentamethyl substitution, which lead to different bonding and charge distribution patterns for Cp vs Cp* ligands in the mixed metallocenes.

Only very few cyclopentadienyl transfer reactions are known.[33] Some examples from the chemistry of nickelocene, as, e.g., the reaction of $[(COD)Rh(solv)_x]^+$ with $NiCp_2$ to give CpRh(COD) and $[Ni_2Cp_3]^+$,[7] seem to be closely related to the work described here. It is tempting to assume that a short-lived triple-decker species [(COD)Rh($\mu$-Cp)NiCp]$^+$ is a key intermediate in this reaction.

Cyclopentadienyl transfer reactions may be of synthetic interest, in particular if a cheap substrate as, e.g., commercially available ferrocene derivatives can be used as starting material for the preparation of otherwise inaccessible or expensive complexes. The preparation of the ruthenium complex $14^+$ illustrates this aspect.

## Experimental Section

Experiments were carried out under dinitrogen using conventional Schlenk techniques. Nitromethane and acetonitrile were dried by filtration through activated basic alumina and distilled in vacuo. Acetone was refluxed over $B_2O_3$ for 24 h and then distilled. NMR spectra were recorded on a Bruker WP-80 SY ($^1$H, 80 MHz) and a Bruker WH-270 ($^{13}$C, 67.88 MHz) instrument. Chemical shifts are relative to internal TMS.

**(Pentamethylcyclopentadienyl)(cyclopentadienyl)ruthenium (1).** NaCp·DME[34] (0.30 g, 1.68 mmol) is added to a suspension of $(RuClCp^*)_4$[35] (0.456 g, 0.42 mmol) in THF (20 mL) at −78 °C. The suspension is stirred and slowly warmed to ambient temperature. The solvent is then removed, and the residue is extracted with hexane (3 × 20 mL). Filtration through alumina (column 2 × 3 cm, 7% $H_2O$), evaporation of the hexane in vacuo, and sublimation of the residue afforded **1** (0.44 g, 87%) as a white crystalline solid. $^1$H NMR (acetone-$d_6$): $\delta$ 4.14 (s, Cp), 1.93 (s, Cp*).

(32) It should be noted that our EH calculations do not allow the assessment of the magnitude of ionic contributions to the overall bond strength between ring ligands and the metal.

(33) Rubezhov, A. Z.; Gubin, S. P. *Adv. Organomet. Chem.* **1972**, *10*, 347; Werner, H. *Fortschr. Chem. Forsch.* **1972**, *28*, 141. Efraty, A. *J. Organomet. Chem.* **1973**, *57*, 1. Garrou, P. E. *Adv. Organomet. Chem.* **1984**, *23*, 95.

(34) Aoyagi, T.; Shearer, H. M. M.; Wade, K.; Whitehead, G. *J. Organomet. Chem.* **1979**, *175*, 21.

(35) Fagan, P. J.; Ward, M. D.; Caspar, J. V.; Calabrese, J. C.; Krusic, P. J. *J. Am. Chem. Soc.* **1988**, *110*, 2981. Fagan, P. J.; Mahoney, W. S.; Calabrese, J. C.; Williams, I. D. *Organometallics* **1990**, *9*, 1843.

**(Pentamethylcyclopentadienyl)(cyclopentadienyl)iron (2).** (a) A suspension of $FeCl_2(THF)_2$ (4.0 g, 15 mmol) in ether (200 mL) is treated with a solution of benzoylacetone (4.3 g, 26.5 mmol) in ether (50 mL) and then with piperidine (2.26 g, 26.5 mmol). After stirring for 1 h, the precipitate of ($[C_5H_{10}NH_2]Cl$) is filtered off. Adding hexane (50 mL) to the filtrate and reducing the volume give a precipitate of $Fe(PhCOCHCOMe)_2$[36] (3.6 g, ca. 70%) as purple crystalline powder. (b) NaCp*[37] (0.51 g, 3.2 mmol) is added to a suspension of $Fe(PhCOCHCOMe)_2$[36] (1.19 g, 3.15 mmol) in THF (20 mL) at −78 °C. The color instantaneously turns blue. After stirring for 15 min, NaCp·DME[34] (0.57 g, 3.2 mmol) is added. The reaction mixture is warmed to ambient temperature with continued stirring and then worked up as described above for 1; a small admixture of $FeCp^*_2$ is oxidatively destroyed during chromatography. Crystallization from ethanol gives **2** (0.74 g, 92%) as an orange-yellow crystalline solid. $^1H$ NMR (acetone-$d_6$): δ 3.65 (s, Cp), 1.89 (s, Cp*). $^{13}C\{^1H\}$ NMR (acetone-$d_6$): δ 80.2 ($Fe(C_5Me_5)$), 71.5 (Cp), 11.4 ($C_5Me_5$).

**(μ-Cyclopentadienyl)bis[(pentamethylcyclopentadienyl)ruthenium] Trifluoromethanesulfonate (4·$CF_3SO_3$).** Trifluoromethanesulfonic acid (0.2 mL) is added with stirring to a solution of **1** (0.36 g, 1.19 mmol) and $[Cp^*Ru(OMe)]_2$[14] (0.33 g, 0.62 mmol) in ether (20 mL). A precipitate forms. The supernatant solution is decanted. The precipitate is washed with ether (5 mL) and then dissolved in $CHCl_3$ (10 mL) (alternatively in 10 mL of THF). After cooling to −40 °C, the product slowly crystallizes to give 4·$CF_3SO_3$·$CHCl_3$ (0.37 g, 38%) as a yellow solid. Anal. Calcd for $C_{27}H_{36}Cl_3F_3O_3Ru_2S$: C, 40.23; H, 4.50. Calcd for $C_{26}H_{35}F_3O_3Ru_2S$: C, 45.47; H, 5.14. Found: C, 41.79; H, 4.51. $^1H$ NMR (acetone-$d_6$): δ 4.47 (s, Cp), 1.90 (s, Cp*). $^{13}C\{^1H\}$ NMR (acetone-$d_6$, −20 °C): δ 87.6 ($C_5Me_5$), 57.7 (Cp), 11.2 ($C_5Me_5$).

**(μ-Cyclopentadienyl)[(pentamethylcyclopentadienyl)iron][(pentamethylcyclopentadienyl)ruthenium] Trifluoromethanesulfonate (5·$CF_3SO_3$).** In the same manner as above $[Cp^*Ru(OMe)]_2$[14] (0.33 g, 0.62 mmol) and **2** (0.31 g, 1.21 mmol) afford 5·$CF_3SO_3$·THF (0.34 g, 39%) as a violet crystalline solid. A satisfactory elemental analysis could not be obtained although the material was spectroscopically (NMR) pure. $^1H$ NMR (acetone-$d_6$): δ 4.22 (s, Cp), 1.95 (s, FeCp*), 1.80 (s, RuCp*). $^{13}C\{^1H\}$ NMR (acetone-$d_6$, −20 °C): δ 87.6 ($Ru(C_5Me_5)$), 81.9 ($Fe(C_5Me_5)$), 56.4 (Cp), 11.2 ($Ru(C_5Me_5)$), 10.2 ($Fe(C_5Me_5)$).

**NMR Tube Experiments.** For the preparation of the metalloelectrophiles a suspension of the corresponding halides in $MeNO_2$-$d_3$ or acetone-$d_6$ was treated with $AgCF_3SO_3$ in a stoichiometric amount and stirred for 10 min. The solution was decanted from the AgCl formed and transferred to an NMR tube. For low temperature measurements the solution was frozen with liquid nitrogen. After addition of the substrate the measurement was taken at the desired temperature.

**(Formylcyclopentadienyl)(hexamethylbenzene)ruthenium Trifluoromethanesulfonate (14·$CF_3SO_3$).** $AgCF_3SO_3$ (0.31 g, 1.21 mmol) is added to a suspension of $[(C_6Me_6)RuCl_2]_2$[38] (0.200 g, 0.30 mmol) in acetone (20 mL). After stirring for 30 min, the reaction mixture is slowly filtered through a frit (G4). $Fe(C_5H_4CHO)_2$ (0.30 g, 1.24 mmol) is added and the solution is kept at ambient temperature for 24 h. Addition of hexane (40 mL) precipitates a raw product which is separated and dissolved in $CHCl_3$ (10 mL). Cooling the solution to −40 °C gives 14·$CF_3SO_3$·$CHCl_3$ (0.26 g, 70%) as white crystals. Anal. Calcd for $C_{20}H_{24}Cl_3F_3O_4RuS$: C, 38.44; H, 3.87. Found: C, 38.95; H, 3.95. $^1H$ NMR (acetone-$d_6$): δ 9.87 (s, CHO), 5.70 and 5.51 (AA′BB′, $C_5H_4CHO$), 2.46 (s, $C_6Me_6$). $^{13}C\{^1H\}$ NMR (acetone-$d_6$): δ 191.2 (CHO), 101.8 ($C_6Me_6$), 91.1 (C-1), 86.0 (C-2/5), 81.7 (C-3/4), 17.5 ($C_6Me_6$). IR (KBr): ν(CO) 1684 $cm^{-1}$.

**Table IV. Crystallographic Data for 4·$CF_3SO_3$·THF**

| | |
|---|---|
| formula | $C_{30}H_{43}F_3O_4Ru_2S$ |
| fw | 758.9 |
| cryst syst | triclinic |
| space group | $P\bar{1}$ (No. 2) |
| *a*, pm | 1284.9(6) |
| *b*, pm | 1291.1(6) |
| *c*, pm | 1127.7(3) |
| α, deg | 114.52(3) |
| β, deg | 101.85(3) |
| γ, deg | 87.58(4) |
| *V*, $nm^3$ | 1.663(2) |
| $d_{calcd}$, $g/cm^3$ | 1.515 |
| *Z* | 2 |
| *F*(000) | 772 |
| μ(Mo Kα), $cm^{-1}$ | 9.97 |
| cryst dimens, mm | 0.4 × 0.2 × 0.2 |
| radiation (λ, pm) | Mo Kα (70.93) |
| monochromator | graphite |
| *T*, K | 293 |
| scan mode | ω |
| scan range, deg | $3 \le \theta \le 25$ |
| total data | 6165 |
| no. of unique obsd data ($I > 2.5\sigma(I)$) | 3527 |
| no. of variables | 387 |
| residuals *R*, $R_w$ | 0.050, 0.056 |
| weighting factor, *w* | $w = 1/\sigma^2(F_o)$ |
| GOF | 1.666 |
| max resid density, e $pm^{-3}$ | $0.6 \times 10^{-6}$ |

**Determination of the Structure of 4·$CF_3SO_3$·THF.** Geometry and intensity data were collected on an Enraf-Nonius CAD4 diffractometer. A summary of crystallographic data, data collection parameters, and refinement parameters is given in Table IV. An empirical absorption correction was applied using ψ scan data.[39] The structure was solved by Patterson and difference Fourier methods.[40] In the final full-matrix refinement, non-hydrogen atoms were refined with anisotropic thermal parameters and hydrogen atoms were included as riding in standard positions (C–H 98 pm). The THF molecule was refined as a rigid group with the same isotropic displacement parameter for all atoms.

**Acknowledgment.** This work was supported by the Deutsche Forschungsgemeinschaft and by the Fonds der Chemischen Industrie.

**Supplementary Material Available:** Listings of crystal data, positional parameters, thermal parameters, and bond lengths (11 pages). Ordering information is given on any current masthead page.

OM930352X

(36) Haider, S. Z.; Khan, M. S.; Khadiza, F. *J. Bangladesh Acad. Sci.* **1978**, *2*, 95; *Chem. Abstr.* **1980**, *93*, 113895j.

(37) Rabe, G.; Roesky, H. W.; Stalke, D.; Pauer, F.; Sheldrick, G. M. *J. Organomet. Chem.* **1991**, *403*, 11.

(38) Bennett, M. A.; Huang, T.-N.; Matheson, T. W.; Smith, A. K. *Inorg. Synth.* **1982**, *21*, 74.

(39) North, A. C. T.; Phillips, D. C.; Mathews, F. S. *Acta Crystallogr.* **1968**, *A24*, 351.

(40) Frenz, B. A. The Enraf-Nonius CAD4 SDP—a real-time system for concurrent X-ray data collection and crystal structure determination. In *Computing in Crystallography*; Schenk, H., Olthof-Hazekamp, R. van Koningsveld, H., Bassi, G. C., Eds.; Delft University Press: Delft, The Netherlands, 1978. SDP-PLUS, Version 1.1, 1984, and VAXSDP, Version 2.2, 1985.